

Original Research Report

Diffuse reflectance patterns in cervical spectroscopy

Nena M. Marín^a, Andrea Milbourne^c, Helen Rhodes^c, Thomas Ehlen^b, Dianne Miller^b,
Lou Benedet^b, Rebecca Richards-Kortum^{a,*}, Michele Follen^c

^aDepartment of Biomedical Engineering, University of Texas, 2501 Speedway Street, University of Texas, Austin, TX 78712, USA

^bCancer Imaging Department, British Columbia Cancer Research Centre, 601 W. 10th Avenue, Vancouver, BC, Canada V5Z 1L3

^cCenter for Biomedical Engineering and the Department of Gynecologic Oncology at the University of Texas M.D. Anderson Cancer Center, 1515 Holcombe Blvd., Box 193, Houston, TX 77030, USA

Available online 13 September 2005

Abstract

Objectives. Our laboratory seeks to develop minimally invasive cost-effective methods to improve screening and detection of curable precursors to cervical cancer. Previously, we have presented pilot studies that assess the diagnostic power of auto-fluorescence and diffuse reflectance spectroscopy. In the present study, we evaluate diffuse reflectance spectra from a comprehensive 850 patient clinical trial to determine its ability to discriminate normal tissue from several grades of abnormal cervical tissue.

Methods. Diffuse reflectance spectra at four source detector separations measured from 549 cervical sites were available for analysis. Three classifiers were implemented: one used spectral data directly as input, a second used simple spectral features such as peak position and intensity, and one used principal component analysis for feature selection. Algorithms were developed and evaluated using leave-one-out cross-validation to classify normal and precancerous cervical tissue. The percentage of samples correctly classified was used to evaluate and compare the performance of the algorithms, as compared to histology.

Results. Diffuse reflectance spectra of cervical precancer showed consistent differences from that of normal tissue at all source detector separations; reflectance intensity of precancer was lower than that of normal tissue on average. Normal cervical tissue spectra show more intensity variation between patients than other tissue grades. Reflectance spectra acquired from the closest source detector separations consistently demonstrated the most relevant information for tissue classification. Two persistent spectral patterns demonstrated that the contribution of hemoglobin absorption and the wavelength-dependent spectral slope contained relevant information for classification.

Conclusions. Spectral patterns in diffuse reflectance spectra can be used for the discrimination of normal cervical tissue from low grade and high grade squamous intraepithelial lesions.

© 2005 Elsevier Inc. All rights reserved.

Keywords: Cervix; Diffuse reflectance spectroscopy; Tissue diagnostics

Introduction

Diffuse reflectance is an optical technology that enables direct quantification of absorption and scattering tissue properties. Dysplastic cells undergo morphometric changes affecting nuclear size, nuclear circumference, nuclear to cytoplasmic ratio, angiogenesis, and fractal dimension, and chromatin texture. These changes alter both absorption and

scattering tissue properties. Several research efforts [1–7] have demonstrated that diffuse reflectance of tissue has the potential to detect these tissue morphometric changes and therefore distinguish between precancerous and normal tissues.

Current screening strategies for cervical intraepithelial neoplasia are based on Pap smears from asymptomatic women. Patients with an abnormal Pap smear are referred for colposcopic evaluation. Based on colposcopy, the patient may be referred for a biopsy, i.e. removal of tissue for histologic evaluation. Current cervical cancer precancer screening histologic classifications include: mild dysplasia

* Corresponding author. Fax: +1 512 475 8854.

E-mail address: kortum@mail.utexas.edu (R. Richards-Kortum).

or CIN (cervical intraepithelial neoplasia) grade 1, moderate dysplasia or CIN 2, severe dysplasia or CIN 3, and carcinoma in situ (CIS).

This paper presents a data discovery study that evaluates the predictive power of diffuse reflectance when compared against histology as the gold standard (truth) for tissue disease state.

Materials and methods

Phase I and II clinical trials to assess technical feasibility of optical technologies for the *in vivo* diagnosis of cervical precancers have been underway in our laboratory for the past 10 years. We have just completed data acquisition in a comprehensive phase II clinical trial to assess the technical efficacy of fluorescence and diffuse reflectance spectroscopy acquired from 850 women at three clinical locations with two research grade optical devices [8,9].

Patient population

Diffuse reflectance spectra from 1507 cervical tissue measurements are available for analysis. Of these 1507, 980 were histologically normal, and 527 were from tissue with some degree of neoplasia based on histologic evaluation. All participants in the study were voluntarily enrolled and consented for spectroscopic, histologic, cytologic, and colposcopic evaluation.

Data processing and structure

Diffuse reflectance was measured at four source detector (SD-*n*) separations ranging from 0.25 to 3 mm separation (see Fig. 1, reflectance channels SD-0, SD-1, SD-2, and SD-3) in the emission range of 370 through 650 nm. Raw reflectance spectra were pre-processed for removal of background signals, wavelength and intensity calibration, and spectral smoothing. Additionally, the spectra were normalized using standard spectra obtained from a solution of 0.625% (vol) of 1.02 μm diameter polystyrene microspheres (Bang Laboratories, Inc., Fishers, IN). After pre-processing, the spectra were reviewed for quality by two independent experts. Spectra containing measurement artifacts were removed from further analysis. Data analyzed were only from patients with quality spectra at all four reflectance SDS. Due to a chip in the tip of the fiber optic probe, we were unable to collect reflectance spectra at SD-0 in a large fraction of the first 250 patients. In the whole study, of the 1507 available sites, 911 sites had high quality spectra from all four sites. The approved spectra were then assembled into a datacube for analysis. The datacube is a 3-dimensional structure with the *z* dimension representing each individual measurement. The *x* and *y* dimensions contain a biographical header record and 113 reflectance emission intensities (370 to 650 in 2.5 nm increments) at each source detector separation. The bio-

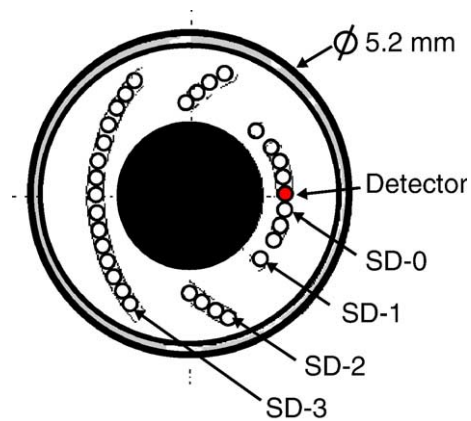


Fig. 1. Characteristics of the fiber optic probe used to collect diffuse reflectance spectra at four source detector separations.

graphical header record contains biographical data about the patient as well as diagnostic gold standard for the measurement based on histology.

Data analysis

The datacube was randomly partitioned into three subsets to be used for training, validation, and testing of implemented algorithms in the approximate proportions of 40%–30%–30% respectively. Each random partitioning was stratified by histology, spectrometer used to acquire the spectra, serum follicle stimulating hormone (FSH) level (menopausal state), and histologic tissue type. For the purposes of this preliminary data discovery analysis, the test set was put aside for a future final algorithm evaluation, and the training and validation sets were combined into a single data set containing a total measurement count of 549 records. The goal was to evaluate the diagnostic power of diffuse reflectance alone under several algorithm input/expected output combinations. The general approach was (1) to classify the spectral data set using leave-one-out cross-validation (LOO) and (2) to calculate a percentage of correctly classified samples.

Algorithms

Principal component analysis/Fisher discriminant analysis algorithm

Principal component analysis (PCA) for feature selection was applied to diffuse reflectance emission spectra for a single reflectance channel (SDS). Fisher discriminant analysis (FDA) was implemented for discrimination based on a binary target (e.g. Class 1: $D_x = 1$ for all sites histologically “negative for dysplasia”, Class 2: $D_x = 0$ for the rest or all sites histologically NOT “negative for dysplasia”). Inputs to the FDA classifier were these principal component scores (PCS) identified as statistically significant using a two-sample *t* test for independent samples ($P < 0.05$), with equality of variance between the two groups ($D_x = 1$ and $D_x = 0$) based upon an *F* test.

Table 1
Histology of samples used for data analysis

Histology	No. of samples
CIS	16
Severe dysplasia (CIN3)	27
Moderate dysplasia (CIN2)	45
Mild dysplasia (CIN1)	46
HPV-associated changes	61
Atypia	82
Negative for dysplasia	272
Total	549

The algorithm

A *k*-nearest neighbor algorithm was implemented with *k* = 1 neighbor for discrimination of a binary target, created by dichotomization of each unique tissue state (e.g. *Dx* = 1 for histologically diagnosed “negative for dysplasia” from *Dx* = 0 for histologically diagnosed as any other category or NOT “negative for dysplasia”). Inputs to the algorithm classifier were the entire emission spectra at a single reflectance source detector separation. The algorithm was implemented using the Euclidean distance to determine the closest neighboring spectra.

In addition to the mentioned classifier inputs, diffuse reflectance spectral characteristics based on shape and intensity were extracted including:

1. Intensity and wavelength at first and last acquired spectral intensity value. These two data points were then

combined into a new feature termed the wavelength-dependent slope.

2. Intensity and wavelength of spectral valleys associated with hemoglobin absorption found between 400 to 450 nm and 525 to 575 nm.
3. Intensity and wavelength of peak found between 490 and 525 nm.
4. Intensity and wavelength of peak found between 575 and 630 nm.

In this data discovery process, two factors were evaluated with both classifiers: (1) the single SDS which yielded best tissue discrimination, (2) which particular disease grade(s) would have the most naturally separable patterns based on spectroscopy.

Results

Reflectance spectra acquired from 549 cervical sites at four source detector separations were available for analysis from 301 patients. These data are part of a comprehensive study, which has accrued a total of 850 patients. Table 1 summarizes the number of samples used in data analysis. We calculated average spectra and standard deviations for each tissue type. Some tissue classifications were found to be more consistent, demonstrating less variation from site to site and patient to

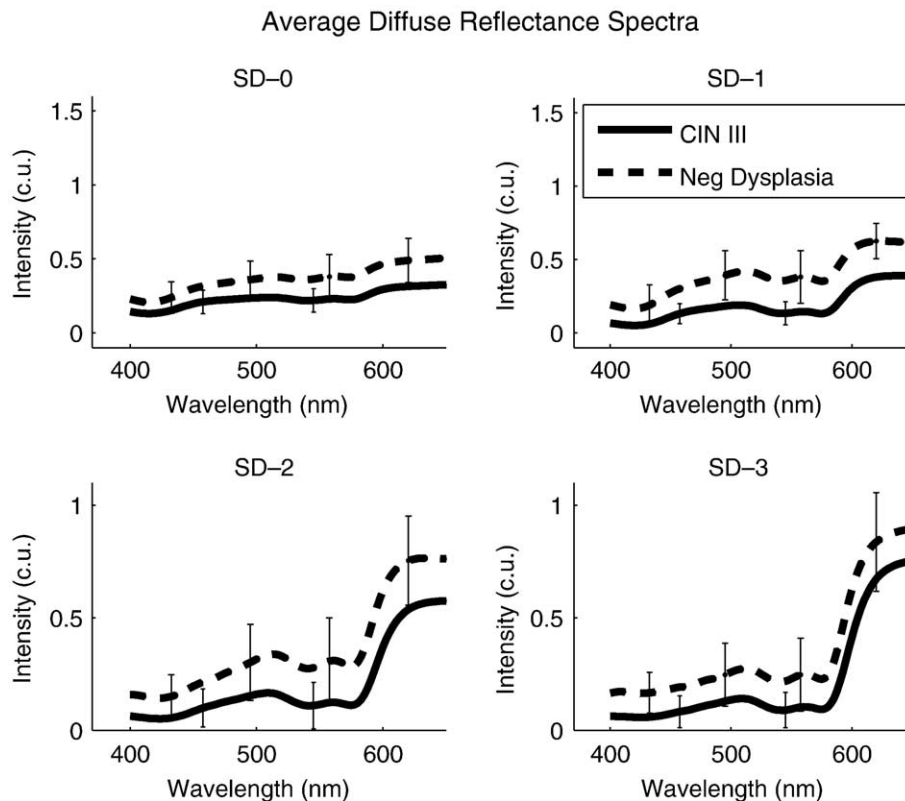


Fig. 2. Average diffuse reflectance spectra comparing histologically normal tissue versus CIN 3.

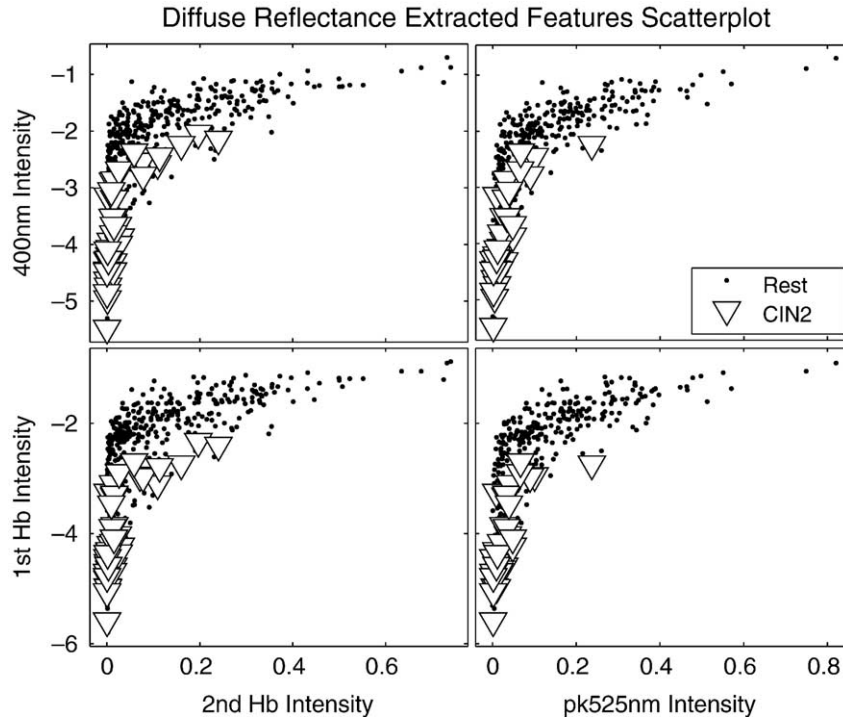


Fig. 3. Scatter plot of extracted spectral features for CIN 2 versus all other tissue types.

patient in spectral intensity and/or shape. Fig. 2 shows the average diffuse reflectance spectra for two histologic tissue grades: CIN 3 and negative for dysplasia. The error bars represent the standard deviation within the averaged samples. The average reflectance intensity of CIN 3 is lower than that of normal tissue at all SDSs. The standard deviation is substantially higher for the normal samples than for CIN 3. Spectra of both CIN 3 and normal tissue show valleys due to hemoglobin absorption at 410–430 nm and 530–590 nm.

Initially, we examined peak intensity, peak location, and spectral slope features for their tissue discrimination ability. Fig. 3 shows scatter plots for four of these spectral features

separating CIN 2 from all other tissue grades in this data set. The intensity at 400 nm, 540 nm, and 580 nm hemoglobin valleys plotted versus the intensity of the 525 nm peak shows good separation for CIN 2 from all other tissue categories.

After applying principal component analysis to the diffuse reflectance measurements, two of the statistically significant principal components could be related to two features in the spectra. Fig. 4 shows the two principal components; the first pattern is most likely the Soret absorption of hemoglobin. The second pattern is related to the wavelength-dependent slope of the spectra at SD-0. The slope corresponds to a line connecting the first

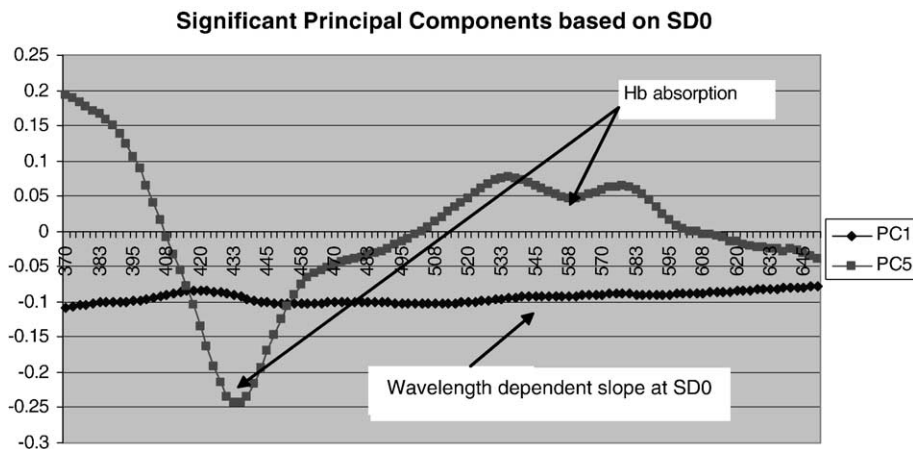


Fig. 4. Patterns of significant principal components at SD0.

Table 2
Comparison of classification accuracy

Dichotomized target	Classifier	% Correct	Channel
Severe dysplasia (CIN 3)	PCA/FDA	98	SD2
Moderate dysplasia (CIN 2)	1NN	94	SD1
Mild dysplasia (CIN 1)	PCA/FDA	93	SD0
Negative for dysplasia	PCA/FDA	73	SD1

intensity to the last intensity in the spectra for one reflectance channel.

Table 2 summarizes the classifier results. The principal component analysis/Fisher discriminant analysis classifier was more effective for classification of various tissue grades than the 1NN classifier. The 1NN classifier was most effective at distinguishing CIN 2 grade with an accuracy of 98%. The consistency of spectral patterns in the CIN 3 grade sites resulted in a classification accuracy of 98%. Source detector separations SD0, SD1, and SD2 consistently contained the most significant patterns for discrimination.

Conclusions

Reflectance acquired from the closest source detector separations consistently demonstrated the most relevant information for tissue classification. Two persistent spectral patterns demonstrated that the contribution of hemoglobin absorption and the wavelength-dependent slope are relevant features for classification. Features extracted directly from spectra showed similar results to patterns found using PCA. Hemoglobin absorption, the intensity at the first acquired wavelength (first point defining the slope), and additionally the 525 nm peak intensity contained most relevant information for tissue classification. Normal cervical tissue spectra show more intensity variation between patients than other tissue grades. Spectral patterns in HG lesions are more consistent than other tissue grades.

Optical spectroscopy using diffuse reflectance in the UV-VIS spectral range contains information relevant to separating normal tissue from several grades of abnormal cervical tissue. Based on these results, future efforts will combine the information extracted from diffuse reflectance with fluorescence spectroscopy towards a classification algorithm

that can effectively and accurately separate precancerous lesions from normal cervical tissue.

Acknowledgments

This research was supported by NIH-NCI Program Project Grant 2P01CA082710-06 “Optical Technologies for Cervical Neoplasia”.

Special thanks to Dizem Arifler, Sylvia Au, Olga Shuhatovich, Roderick Price, Brian Pikkula, Ulrich Stange, Robert Knight, the doctors, nurses, and clinical staff at the U.T. M.D. Anderson Cancer Center in Houston, the Lyndon B. Johnson Harris County Hospital District in Houston, the British Columbia BC Cancer Agency, and the Vancouver General Hospital Women’s Clinic in Vancouver.

References

- [1] Bigio IJ, Loree TR, Mourant J. Spectroscopic diagnosis of bladder cancer with elastic light scattering. *Lasers Surg Med* 1995;16:350–7.
- [2] Mourant JR, Freyer JP, Hielscher AH, Eick AA, Shen D, Johnson TM. Mechanisms of light scattering from biological cells relevant to noninvasive optical-tissue diagnostics. *Appl Opt* 1998;37:3586–93.
- [3] Georgakoudi I, Sheets E, Müller M, Backman V, Crum C, Badizadegan K, et al. Trimodal spectroscopy for the detection and characterization of cervical precancers in vivo. *Am J Obstet Gynecol* 2002;186:374–82.
- [4] Arifler D, Guillard M, Carraro A, Malpica A, Follen M, Richards-Kortum R. Light scattering from normal and dysplastic cervical cells at different epithelial depths: finite-difference time-domain modeling with a perfectly matched layer boundary condition. *J Biomed Opt* 2003;8:484–94.
- [5] Drezek R, Guillard M, Collier T, Boiko I, Malpica A, Macaulay C, et al. Light scattering from cervical cells throughout neoplastic progression: influence of nuclear morphology, DNA content, and chromatin texture. *J Biomed Opt* 2003;8:7–16.
- [6] Breslin TM, Xu F, Palmer GM, Zhu C, Gilchrist KW, Ramanujam N. Autofluorescence and diffuse reflectance properties of malignant and benign breast tissues. *Ann Surg Oncol* 2004;11(1):65–70.
- [7] deVeld D, Skurichina M, Witjes M, Duin R, Sterenborg H, Roodenburg J. Autofluorescence and diffuse reflectance spectroscopy for oral oncology. *Lasers Surg Med* 2005;36:356–64.
- [8] Mirabal YN, Chang SK, Atkinson EN, Malpica A, Follen M, Richards-Kortum R. Reflectance spectroscopy for in vivo detection of cervical precancer. *J Biomed Opt* 2002;7:587–94.
- [9] Chang SK, Follen M, Malpica A, Utzinger U, Staerker G, Cox D, et al. Optimal excitation wavelengths for discrimination of cervical neoplasia. *IEEE Trans Biomed Eng* 2002;49:1102–11.